Original Paper

Exergetic analysis for optimization of a rotating equilateral triangular cooling channel with staggered square ribs

Mi-Ae Moon[1] and Kwang-Yong Kim[2]

[1,2]Department of Mechanical Engineering, Inha University
253 Yonghyun-Dong, Incheon, 402-751, Republic of Korea, kykim@inha.ac.kr

Abstract

Exergetic analysis was introduced in optimization of a rotating equilateral triangular internal cooling channel with staggered square ribs to maximize the net exergy gain. The objective function was defined as the net exergy gain considering the exergy gain by heat transfer and exergy losses by friction and heat transfer process. The flow field and heat transfer in the channel were analysed using three-dimensional Reynolds-averaged Navier-Stokes equations under the uniform temperature condition. Shear stress transport turbulence model has been selected as a turbulence closure through the turbulence model test. Computational results for the area-averaged Nusselt number were validated compared to the experimental data. Three design variables, i.e., the angle of rib, the rib pitch-to-hydraulic diameter ratio and the rib width-to-hydraulic diameter ratio, were selected for the optimization. The optimization was performed at Reynolds number, 20,000. Twenty-two design points were selected by Latin hypercube sampling, and the values of the objective function were evaluated by the RANS analysis at these points. Through optimization, the objective function value was improved by 22.6% compared to that of the reference geometry. Effects of the Reynolds number, rotation number, and buoyancy parameter on the heat transfer performance of the optimum design were also discussed.

1. Introduction

For internal cooling of turbine blades in gas turbine engine, various turbulators, such as ribs, pin-fins, dimples and protrusions, are employed to enhance the forced convection heat transfer by promoting turbulence production. Among many kinds of turbulators, ribs are one of the best turbulators to enhance the heat transfer by enlarging the heat transfer area and interrupting the boundary layer as well as promoting the generation of turbulent kinetic energy.

There have been many researches to investigate the heat transfer enhancement by the ribs in cooling channels [1-3]. Han [1] experimentally studied the heat transfer and friction factor in various rectangular channels with ribs on the heated surfaces with different channel aspect ratios (ARs=1:4, 1:2, 1:1, 2:1 and 4:1). Their results indicated that the narrow aspect ratio channels (ARs=1:4, 1:2 and 1:1) showed a larger increment in the heat transfer performance than the wide aspect ratio channels (ARs=2:1 and 4:1). Chandra et al. [2] experimentally studied the heat transfer and pressure drop in a square channel with ribs. They reported that the heat transfer enhancement increased as the number of ribbed walls increased while the pressure loss also increased under the same conditions. Islam et al. [3] performed an experimental study to investigate the effects of the Reynolds number and the pitch-to-hydraulic diameter ratio on the heat transfer performance. Their results indicated that the heat transfer augmentation and pressure drop in the ribbed channel increased as the Reynolds number and the pitch-to-hydraulic diameter ratio increased.

The high-speed rotation of turbine blades makes complexities in the flow and temperature fields in the internal cooling passages. When the coolant flows through a rotating cooling channel, it experiences the Coriolis force. The Coriolis force mainly generates the asymmetric secondary flows in the internal cooling passages and acts as a source term in the momentum conservation equations to generate vortices. Coriolis-induced secondary flows make a difference in heat transfer distribution between the leading (suction) and trailing (pressure) sides of the internal cooling passages. Murata and Mochizuki [4] numerically studied the effect of channel rotation on the heat transfer in a two-pass square channel with 180° sharp turns using LES simulation. Their results showed that the heat transfer performance was dominated by the 180° sharp turns and the channel rotation. Since the direction of Coriolis force induced by the channel rotation was different between the 1st and 2nd passages, the trailing surface in the

1st pass and the leading surface in the 2nd pass showed higher heat transfer rates than the others. Wright *et al*. [5] investigated the heat transfer performance in a rotating narrow rectangular internal cooling channel. They concluded that the rotation was the more dominant factor in the heat transfer performance than the cooling channel geometry. Liu *et al*. [6] experimentally conducted the rotation effect on the heat transfer in a two-pass rectangular channel. They concluded that increasing the Rotation number increased the Nusselt number on the trailing surface, but decreased the Nusselt number on the leading surface in the first passage. And, this tendency was reversed in the second passage of the two-pass internal cooling channel.

The previous studies dealt with the rectangular internal cooling channel, but the cooling channel installed in the leading edge of turbine blade usually takes the shape of triangle as shown in Fig. 1. Because of triangular shape, the flow field and temperature distribution are different from those of the rectangular channel. Metzger and Vedular [7] experimentally measured the heat transfer coefficients in triangular channels with angled ribs (30°, 45° and 60°) on two walls under the stationary condition. They reported that the cooling channel with 60° angled rib provided the best heat transfer enhancement among the tested cases. Dutta *et al*. [8] investigated the heat transfer coefficients in a two-pass rotating triangular channel for various orientations to the direction of rotation. They found that the rotation of triangular channel increased the Nusselt number on the trailing surface and decreased the Nusselt number on the leading surface. Liu *et al*. [9] experimentally measured the heat transfer coefficients in an equilateral triangular internal cooling channel for various Reynolds numbers and rotation numbers. The results from this study showed that the heat transfer rate on the trailing surface enhanced as the Reynolds number and rotation number increased.

In general, the convective heat transfer by forced convection leads to pressure drop in heat transfer devices, which causes considerable exergy loss. Thus, the heat transfer and exergy loss are interrelated from a thermodynamical point of view. In the previous works [10, 11] for optimizations of heat transfer augmentation devices, the objective functions related to the heat transfer and friction loss were linearly combined with a weighting factor to constitute a mono-objective function. In that case, the weighting factor should be determined by the designer considering energy economy of the system to be designed. Since the weight factor had to depend on the designer's experience, it was inevitable that the value of objective function was inaccurate. However, recently, Lee and Kim [12] proposed a theoretical approach to compromise between enhancement of heat transfer and friction loss by introducing exergy loss analysis. There have been also some other studies [13, 14] on heat exchanging devices using exergy analysis. Prasad and Shen [13] evaluated the heat transfer augmentation device using exergy analysis to reduce the exergy destruction. Cornelissen and Hirs [14] tried to optimize a heat exchanging system based on a new method which combines exergy analysis and life cycle analysis. They concluded that the new method gives better performance for heat exchanger which leads to the lowest life cycle irreversibility.

The surrogate models being widely used in multidisciplinary optimization have an advantage in accurately representing the characteristics of the design space with improved computational economy [15]. Among various surrogate models, the Kriging method [16] has been widely used for approximate deterministic computer models as it provides the best linear unbiased predictor. Kim and Moon [10] performed the numerical optimization of stepped circular arrays using Kriging method [19] to enhance the heat transfer performance.
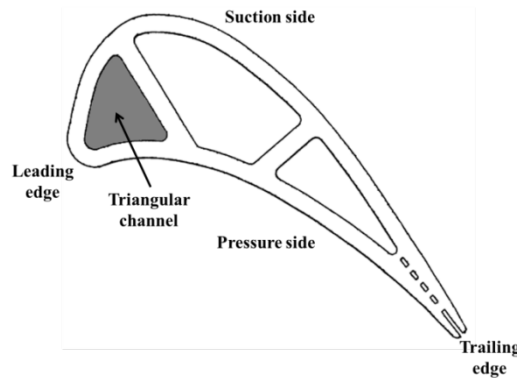

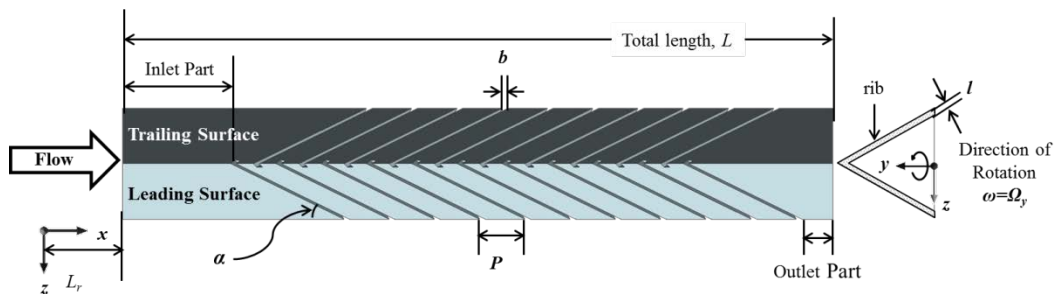**Fig. 1** Internal cooling channels in the gas turbine blade

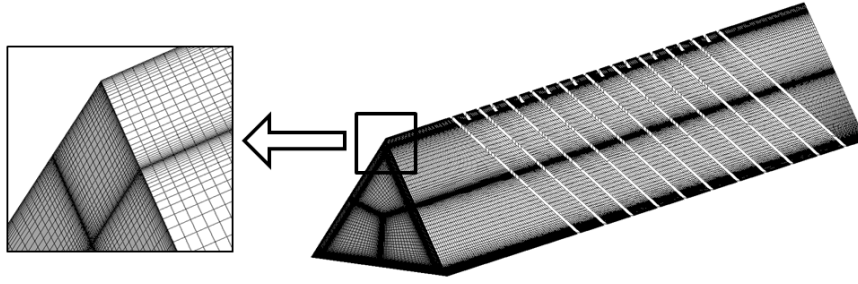**Fig. 2** Computational domain and geometric parameters [11]

230

Fig. 3 Example of grid system [11]

In the present work, exergy analysis was introduced in optimization of a triangular channel with staggered square ribs, which is located at the leading part of a turbine blade where heavy heat load occurs, to maximize the net exergy gain in the channel using three-dimensional Reynolds-averaged Navier-Stokes (RANS) equations. Design points with three design variables were selected using Latin hypercube sampling (LHS) [17]. Kriging (KRG) meta-modelling techniques [16] were used to construct surrogate model for the objective function of the optimization.

2. Numerical Analysis

Geometry of the cooling channel considered in this work is shown in Fig. 2 which was presented in the previous study [11]. The hydraulic diameter (D_h) of the reference channel is 18.3mm, which is same as that used by Liu *et al.* [9]. The three sides of the triangle are equal in length as 31.8mm. The distance from the inlet of channel to rotation axis (z-axis) is L_r=38.2mm. The total length of the channel (L) is 215mm. The eleven ribs are placed on the leading surface of the channel as in the work of Liu *et al.* [9], and ten ribs on the trailing surface. The ribs are installed obliquely to the mainstream flow and the angle of attack (α) is 45° as shown in Fig. 2, same as in the experimental study of Liu *et al.* [9] and the reference study of Park *et al.* [11]. The smooth surface where the ribs are not installed is denoted as the bottom surface. In the reference channel, the rib pitch-to-hydraulic diameter ratio (P/D_h) is 0.696, and the rib width-to-hydraulic diameter ratio (b/D_h) and the rib height-to-hydraulic diameter ratio (l/D_h) have the same value as 0.087. The inlet and outlet parts of the channel indicated in Fig. 2 have the lengths, 30.5mm and 9.7mm, respectively. The Reynolds number based on the channel hydraulic diameter was fixed at 20,000. The working fluid (coolant) was the compressed pure air which is extracted from the 2nd~ 5th stages of compressor. As boundary conditions, the inlet total temperature of coolant flow was kept constant as 296.15K and the constant velocity was used at the inlet. A total pressure was fixed at the outlet of the channel. The Rotation number ($Ro=\Omega_y D_h/U$) of the channel was 0.28, as in the work of Liu *et al.* [9]. A constant temperature (338.15K) was adopted on the leading and trailing surfaces including the rib surface (Fig. 2), and adiabatic and no-slip conditions were used on the bottom surface.

In present study, three-dimensional RANS analyses of the fluid flow and convective heat transfer were performed using ANSYS-CFX 11.0 [18]. And, ANSYS ICEM 11.0 was used to construct a hexahedral grid for the numerical analysis. Fig. 3 shows

Table 1 Design variables and design space [11]

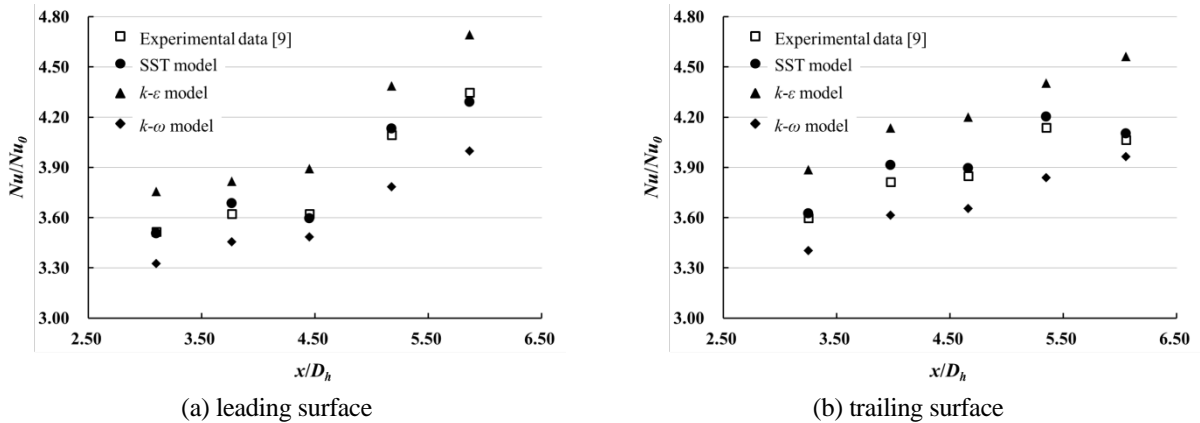| Design variables	Lower bound	Upper bound
α (°)	30.0	90.0
P/D_h	0.522	0.696
b/D_h	0.0546	0.1093

(a) leading surface

(b) trailing surface

Fig. 4 Comparison between measured and calculated Nusselt number ratios
on the heated surfaces with different turbulence models [11]

an example of the computational grids used in this work. The grids are concentrated at the wall region to resolve the high velocity gradient.

In this study, a high-resolution scheme that is second-order accurate in space was used to solve the convection-diffusion equations. The three-dimensional steady RANS equations were solved using the shear stress transport (SST) turbulence model [19] with automatic wall treatment. The SST model combines the advantages of the k-ω [20] and the k-ε [21] models with a blending function. The k-ω model was activated in the near-wall region, and the k-ε model was used in the other region. Bardina *et al*. [22] suggested that the SST model captures the flow separation under an adverse pressure gradient more effectively than other eddy viscosity models. Thus, this model is expected to more accurately predict the near-wall turbulence, which is important in the accurate prediction of turbulent heat transfer in the coolant channel. The grid points adjoining the wall are placed at y^+ less than 2.0 to apply low-Reynolds- number SST model [19].

The convergence criterion for the root-mean-square residual values for all flow parameters was set to 1.0×10^{-5} and the momentum and energy imbalances in the entire computational domain assured less than 3.97%. And, relative changes of the temperature and velocity values in the region between the staggered ribs, were measured to check the uncertainty, and less than 1.47%.

3. Optimization Method

The objective function of the optimization was defined as net exergy gain considering the exergy gain by heat transfer, and exergy losses by friction and heat transfer process following the work of Lee and Kim [12] for dimpled channel, as follows:

$$F = \dot{E}_{gain} - \dot{E}_{loss} \tag{1}$$

Table 2 Experimental designs and their objective function values

Design Point	Design variables			Objectives		
	α (°)	P/D_h	b/D_h	$\dot{E}_{gain}$	$\dot{E}_{loss}$ by friction	$\dot{E}_{loss}$ by heat transfer
1	52.857	0.688	0.075	10.614	1.012	1.028
2	30.000	0.638	0.109	9.835	3.126	2.415
3	64.286	0.630	0.086	14.046	2.711	1.823
4	81.429	0.580	0.101	11.815	0.974	0.935
5	38.571	0.530	0.068	10.162	0.713	3.152
6	35.714	0.679	0.070	6.782	1.922	2.523
7	75.714	0.646	0.055	9.991	1.523	1.886
8	78.571	0.671	0.099	15.162	3.934	1.900
9	44.286	0.522	0.083	10.962	2.014	2.412
10	90.000	0.547	0.060	11.041	2.412	1.002
11	67.143	0.597	0.096	10.005	3.007	0.986
12	41.429	0.613	0.078	8.936	0.995	0.824
13	84.286	0.655	0.088	7.124	1.294	1.472
14	87.143	0.605	0.062	6.081	1.763	1.991
15	58.571	0.621	0.057	7.933	2.815	1.241
16	61.429	0.588	0.081	8.992	2.005	2.830
17	55.714	0.663	0.091	9.815	1.024	1.640
18	50.000	0.572	0.104	10.962	0.837	2.916
19	32.857	0.539	0.094	13.245	1.256	3.012
20	72.857	0.563	0.065	16.026	3.734	3.823
21	70.000	0.696	0.107	7.625	2.173	0.815
22	47.143	0.555	0.073	14.915	1.623	3.316

Table 3 Results of optimization

	Design variables			Objectives			
	α (°)	P/D_h	b/D_h	$\dot{E}_{gain}$	$\dot{E}_{loss}$ by friction	$\dot{E}_{loss}$ by heat transfer	F
Reference	45.0	0.696	0.087	10.812	1.035	1.684	8.093
Optimum-A	30.4	0.554	0.093	12.438	1.081	1.435	9.922
Optimum-B [11]	46.6	0.638	0.098	11.892	1.097	1.523	9.282

(a) Reference design
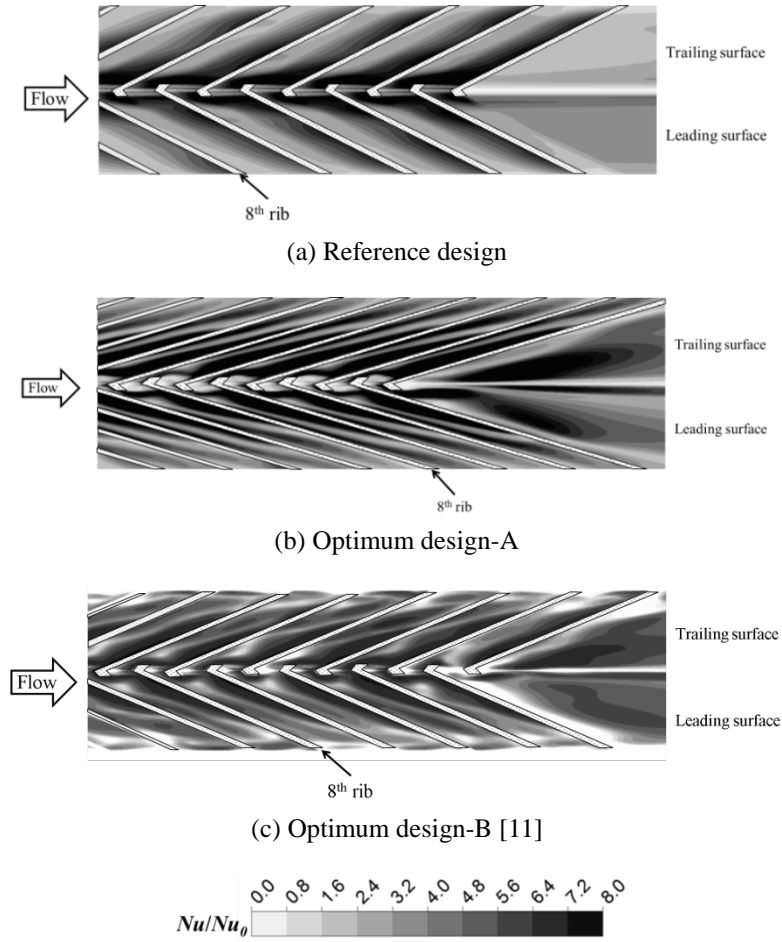

(b) Optimum design-A

(c) Optimum design-B [11]

Fig. 5 Nusselt number distributions on the heated surfaces at Re=20,000

where $\dot{E}_{gain}$ indicates the exergy obtained by heat transfer. Under the condition of constant temperature at the heat transfer surface, the exergy gain is represented as follows:

$$\dot{E}_{gain} = \left(1 - \frac{T_0}{T_1}\right)\dot{Q} \tag{2}$$

where $\dot{Q}$ is the total heat transfer rate in the cooling channel, and T_0 and T_1 are the environment and wall temperatures, respectively.

The exergy loss by friction and heat transfer can be written as

$$\dot{E}_{loss} = \left(1 - \frac{T_0}{T_2}\right)\dot{Q} + \Delta p \frac{\dot{m}}{\rho}\left(\frac{T_0}{T_2}\right) \tag{3}$$

where T_2 is the coolant flow temperature, Δp is the pressure drop through the channel, $\dot{m}$ is the mass flow rate of the flow, and ρ is fluid density. The first and second terms on the right hand side represent the exergy losses by heat transfer and friction, respectively.

The definitions of geometric parameters are indicated in Fig. 2. From these geometric parameters, four dimensionless parameters, i.e., angle of rib α, the rib pitch-to-hydraulic diameter ratio P/D_h, the rib width-to-hydraulic diameter ratio b/D_h, and the rib height-to-hydraulic diameter ratio l/D_h, can be defined. Among these dimensionless parameters, α, P/D_h, and b/D_h were selected as design variables in this optimization. And, l/D_h was fixed as 0.087 as suggested by Liu *et al*. [9]. Table 1 presents the ranges of design variables for the optimization procedure.

The Kriging model [16] is implemented in applications that involve spatially and temporally correlated data. This model belongs to the family of linear least squares estimation algorithms. The Kriging model combines a global model with localized departure. If $y(x)$ is the unknown function of interest, then according to the Kriging model, $y(x)$ is given by:

$$y(x) = F(x) + Z(x) \tag{4}$$

where $F(x)$ and $Z(x)$ represent the global model and localized deviation, respectively, and $Z(x)$ is the realization of a stochastic process with a zero mean and nonzero covariance. The global model is a linear polynomial function, and the systematic departure
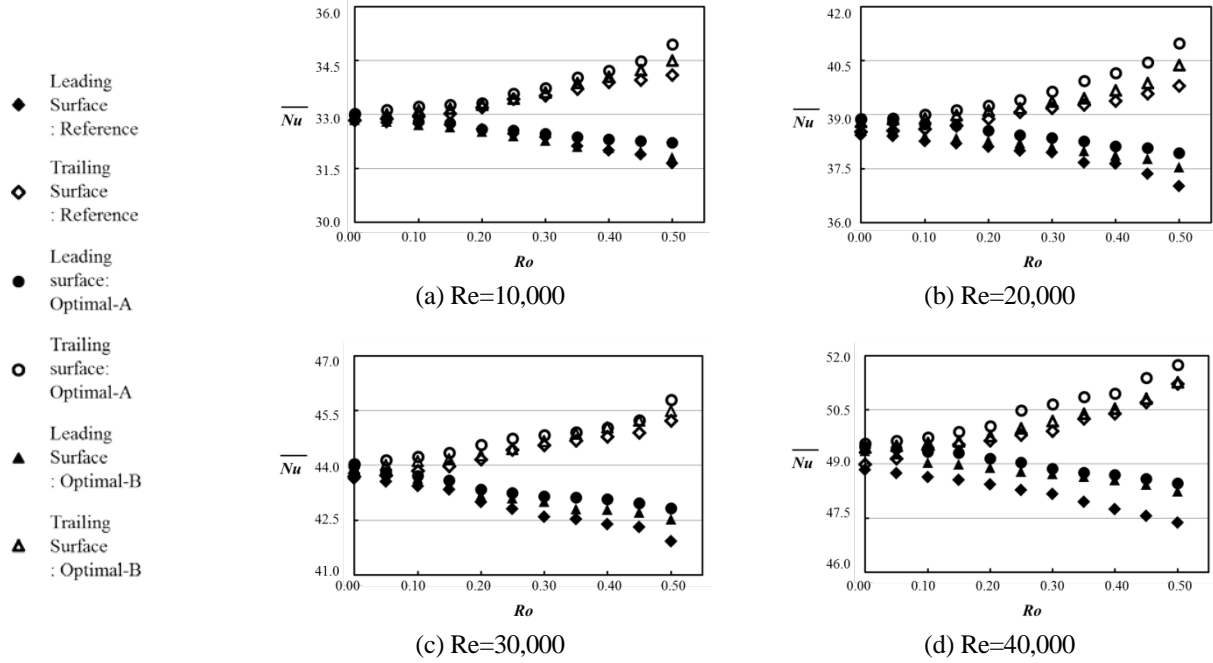
Fig. 6 Variations of area-averaged Nusselt number with rotation number
for different Reynolds numbers

terms follow a Gaussian correlation function. The covariance matrix of $Z(x)$ is given by:

$$\mathrm{cov}[Z(x^i), Z(x^j)] = \sigma^2 \Re[R(x^i, x^j)] \quad i, j = 1, 2, \cdots, n_s \tag{5}$$

where $\Re$ is a correlation matrix consisting of a spatial correlation function $R(x^i, x^j)$ as its elements; σ^2 is the process variance representing the scalar of the spatial correlation function; and $R(x^i, x^j)$ quantifies the correlation between any two of the sampled n_s data points x^i and x^j, and thereby controls the smoothness of the Kriging model, the effect of nearby points, and the differentiability of the surface. The Kiriging model was constructed using the objective function values at the design points selected by LHS [17].

4. Results and Discussion

The grid independency was evaluated by testing different grid systems for the triangular channel with reference ribs in the previous work [11]. Through the grid independency test, the optimal number of grids for the reference ribs was determined to be approximately 6,090,000. The grid systems for the various designs evaluated in this study were constructed with approximately same grid spacing with this optimum grid system for the reference case.

The results of RANS analysis were validated in comparison with the experimental data, which were obtained by Liu *et al.* [9], for the area-averaged Nusselt number distributions on the heated surfaces, in the previous work [11] as shown in Fig. 4. This figure also compares the results calculated by three different turbulence models, i.e., *k-ε*, *k-ω,* and SST turbulence models. The Nusselt number distributions calculated by SST model were close to the experimental data with maximum relative error of only 2.63%, while the *k-ε* and *k-ω* models failed to predict the correct level of the Nusselt number.

Table 2 presents twenty design points selected by LHS and the objective function values calculated at these design points. The values of the design variables and the objective function for the optimum design for the reference and the optimal designs are shown in Table 3. The optimal design-A is the optimal design obtained from the exergy analysis in the present work, while the optimal design-B is that obtained in the previous work [11] using a linear combination of Nusselt number and friction factor as the objective function. The optimal design-A shows the exergy gain by heat transfer increased by 15.0%, the exergy loss by friction increased by 4.4%, and the exergy loss by heat transfer decreased by 14.8%, compared to the reference design. And, the objective function value (*F*) of the optimal design, i.e., net exergy gain, is increased by 22.6 %, compared to the reference design [9]. The optimum design-A presents the exergy gain by heat transfer increased by 4.59%, and the exergy losses by friction and heat transfer decreased by 1.46% and 5.78%, respectively, compared with the optimum design-B[11]. Distributions of local Nusselt number on both heated surfaces for the reference geometry and optimal design-A and B are shown in Fig. 5. The highest Nusselt number takes place in front of each rib. For all cases, the heat transfer coefficient decreases abruptly just behind each rib due to the flow separation, and gradually increases downstream to reach the maximum near the reattachment line. The optimum geometry-A presents larger area of high heat transfer region than the reference geometry and optimum design-B. The rotation of channel creates a thinner boundary layer on the trailing surface, which causes the value of the Nusselt number on the trailing surface slightly higher than that on the leading surface.

Area-averaged Nusselt numbers for various Reynolds and rotation numbers for the reference and optimum designs are presented in Fig. 6. It is found that the Nusselt number is very sensitive to the rotation number. The heat transfer rates on the trailing surface are more enhanced than that on the leading surface. The difference in Nusselt number between the leading and
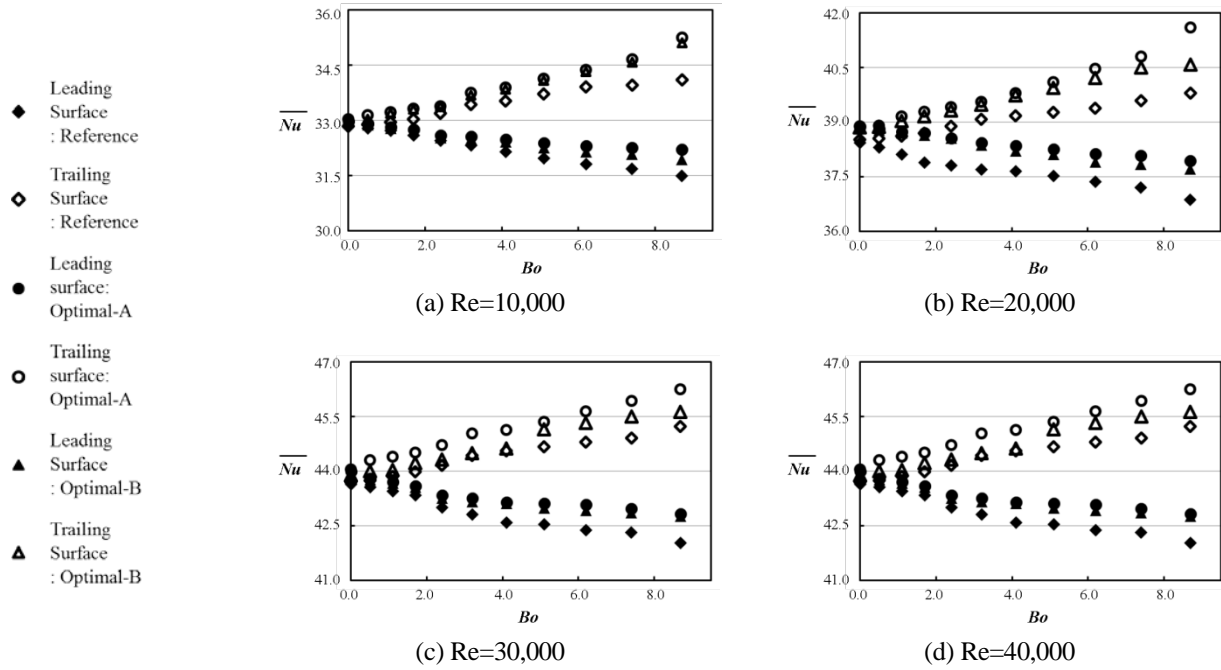
234

Fig. 7 Variations of area-averaged Nusselt number with buoyancy parameter
for different Reynolds numbers

(a) Re=10,000   (b) Re=20,000   (c) Re=30,000   (d) Re=40,000

trailing surfaces increases as the rotation number increases for whole range of Reynolds numbers. The values of Nusselt number for optimal design-A are higher than those for the reference design and optimal design-B over the whole ranges of Reynolds and rotation numbers.

The buoyance parameter (Bo) defined by Wagner *et al*. [24], is generally used as a non-dimensional parameter to evaluate the quantitative combination effect of the temperature difference and Coriolis force:

$$Bo = \left[\frac{T_2 - T_1}{(T_1 + T_2)/2}\right] Ro^2 (L_r/D_h) \tag{6}$$

Variations of area-averaged Nusselt number on the heated surface with the buoyancy parameter for different Reynolds numbers are shown in Fig. 7. The trend of the variations with the buoyancy parameter is similar to that with the rotation number shown in Fig. 6. It is observed that the difference in the heat transfer coefficient between the leading and trailing surfaces is enlarged with the increasing buoyancy parameters for various Reynolds numbers. The increment of buoyancy parameter causes the Nusselt number increase on the trailing surface, and this trend is reversed on the leading surface for both designs. The area-averaged Nusselt number with the optimal design-A is improved in comparison with those of the reference geometry and optimal geometry-B over whole range of buoyancy parameter.

5. Conclusion

An optimization of a rotating triangular cooling channel with staggered ribs under isothermal surface condition was performed based on the exergetic analysis using three-dimensional RANS analysis. The numerical predictions with SST turbulence model gave better agreements with experimental data for the heat transfer coefficient than those with k-ε and k-ω models. The objective function for the optimization was defined by net exergy gain which includes exergy gain by heat transfer and exergy losses by friction and heat transfer. Thus, the objective function is capable of compromising between heat transfer enhancement and friction loss, which is an intrinsic problem in design of heat exchangers. The optimum geometry-A obtained from the present exergetic analysis presented the exergy gain by heat transfer increased by 15.0%, the exergy loss by friction increased by 4.4%, and the exergy loss by heat transfer decreased by 14.8%, and thus the objective function, i.e., net exergy gain improved by 22.6% compared to the reference geometry. The optimum case-A also showed the exergy gain by heat transfer increased by 4.59%, and the exergy losses by friction and heat transfer decreased by 1.46% and 5.78%, respectively, compared with the optimum design-B obtained in the previous work [11]. Through a comparison of the area-averaged Nusselt number among the reference and optimum design-A and B, the optimal design-A showed enhanced area-averaged Nusselt number for the leading and trailing surfaces for all Reynolds numbers, rotation numbers, and buoyancy parameters.

Nomenclature

A_c	Cross sectional area of channel [mm^2]	P	Pitch of the rib [mm]
A_h	Heated surface [mm^2]	Δp	Pressure drop in a channel [Pa]
AR	Aspect ratio	$\dot{Q}$	Heat transfer rate [rad/s]
Bo	Buoyancy parameter	Re	Reynolds number, UD_h/v

b	Width of the rib [mm]		Ro	Rotation number, $\Omega_y D_h/U$
D_h	Hydraulic diameter [mm]		T	Local temperature [K]
$\dot{E}$	Exergy transfer rate [W]		T_0	Reference temperature [K]
F	Objective function		T_1	Wall temperature [K]
f	Friction factor		T_2	Fluid temperature [K]
h	Heat transfer coefficient [W/m²K]		U	Average axial velocity at the inlet [m/s]
k	Fluid thermal conductivity [W/mK]		ω_f	Weighting factor
L	Total length of channel [mm]		x, y, z	Orthogonal coordinate system
L_r	Distance from the inlet of channel to rotation axis [mm]		Ω	Rotation speed [rad/s]
			α	Angle of the rib [°]
l	Height of the rib [mm]		v	Kinetic viscosity [kg/ms]
$\dot{m}$	Mass flow rate [kg/s]		ρ	Fluid density [kg/m³]
Nu	Area-averaged Nusselt number			

References

[1] Han, J. C., 1988, "Heat Transfer and Friction Characteristics in Rectangular Channels with Rib Turbulators," ASME Journal of Heat Transfer, Vol. 110, pp. 321-328.

[2] Chandra, P. R., Alexander, C. R. and Han, J. C., 2003, "Heat Transfer and Friction Behavior in Rectangular Channels with Varying Number of Ribbed Walls," International Journal of Heat and Mass Transfer, Vol. 46, pp. 481-495.

[3] Islam, M. S., Haga, K., Kaminaga, M., Hino, R. and Monde, M., 2002, "Experimental Analysis of Turbulent Flow Structure in a Fully Developed Rib-Roughened Rectangular Channel with PIV," Experiments in Fluids, Vol. 33, pp. 296-306.

[4] Murata, A. and Mochizuki, S., 2004, "Effect of Rib Orientation and Channel Rotation on Turbulent Heat Transfer in a Two-Pass Square Channel with Sharp 180° Turns Investigated by Using Large Eddy Simulation," International Journal of Heat and Mass Transfer, Vol. 47, pp. 2599-2618.

[5] Wright, L. M., Fu, W. L. and Han, J. C., 2005, "Influence of Entrance Geometry on Heat Transfer in Rotating Rectangular Cooling Channels (AR=4:1) with Angled Ribs," Journal of Heat Transfer, Vol. 127, pp. 378-387.

[6] Liu, Y. H., Huh, M., Han, J. C. and Chopra, S., 2008, "Heat Transfer in a Two-Pass Rectangular Channel (AR=1:4) under High Rotation Numbers," Journal of Heat Transfer, Vol. 130, 081701(1-9).

[7] Metzger, D. E. and Vedula, R. P., 1987, "Heat Transfer in Triangular Channels with Angled Roughness Ribs on Two Walls," Experimental Heat Transfer, Vol. 1, pp. 31-44.

[8] Dutta, S., Han, J. C. and Lee, C. P., 1995, "Experimental Heat Transfer in a Rotating Triangular Duct: Effect of Model Orientation," ASME Journal of Heat Transfer, Vol. 117, pp. 1058-1061.

[9] Liu, Y. H., Huh, M., Rhee, D. H., Han, J. C. and Moon, H. K., 2008, "Heat Transfer in Leading Edge, Triangular Shaped Cooling Channels with Angled Ribs under High Rotation Numbers," Proceedings of ASME Turbo Expo 2008, GT2008-50334.

[10] Kim, K. Y. and Moon, M. A., 2009, "Optimization of a Stepped Circular Pin-Fin Array to Enhance Heat Transfer Performance," Heat and Mass Transfer, Vol. 46, pp. 63-74.

[11] Moon, M. A., Park, M. J. and Kim, K. Y., 2013, "Shaped Optimization of Staggered Ribs in a Rotating Equilateral Triangular Cooling Channel," Heat and Mass Transfer, Vol. 50, pp. 533-544.

[12] Lee, K. D. and Kim, K. Y., 2012, "Objective Function Proposed for Optimization of Convective Heat Transfer Devices," International Journal of Heat and Mass Transfer, Vol. 55, pp. 2792-2799.

[13] Prasad, R. C. and Shen, J., 1993, "Performance Evaluation of Convective Heat Transfer Enhancement Devices Using Exergy Analysis," International Journal of Heat and Mass Transfer, Vol. 36, pp. 4193-4197.

[14] Cornelissen, R. L. and Hirs, G. G., 1997, "Exergetic Optimisation of a Heat Exchanger," Energy Conservation and Management, Vol. 38, pp. 1567-1576.

[15] Samad, A. and Kim, K. Y., 2009, "Surrogate Based Optimization Techniques for Aerodynamic Design of Turbomachinery," International Journal of Fluid Machinery Systems, Vol. 2, pp. 179-188.

[16] Martin, J. D. and Simpson, T. W., 1989, "Use of Kriging Models to Approximate Deterministic Computer Models," AIAA Journal, Vol. 4, pp. 853-863.

[17] MP. Software Package, 2004, Ver. 5.1 SAS Inst. Inc., Cary, NC.

[18] ANSYS CFX-11.0, 2006, ANSYS Inc.

[19] Menter, F. R., 1994, "Two-Equation Eddy-Viscosity Turbulence Models for Engineering Applications," AIAA Journal, Vol. 32, pp. 1598-1605.

[20] Launder, B. E. and Spalding, D. B., 1974, "The Numerical Computation of Turbulent Flows," Computer Methods in Applied Mechanics and Engineering, Vol. 3, pp. 269-289.

[21] Wilcox, D. C., 1998, "Reassessment of the Scale-Determining Equation for Advanced Turbulence Models," AIAA Journal, Vol. 26, pp. 1299-1310.

[22] Bardina, J. E., Huang, P. G. and Coakley, T. J., 1997, "Turbulence Modelling Validation, Testing, and Development," NASA Technical Memorandum, 110446.

[23] Gee, D. L. and Webb, R. L., 1980, "Forced Convection Heat Transfer in Helically Rib-Roughened Tubes," International Journal of Heat and Mass Transfer, Vol. 23, pp. 1127-1135.

[24] Wagner, J. H., Johnson, B. V. and Hajek, T. J., 1991, "Heat Transfer in Rotating Passage with Smooth Walls and Radial Outward Flow," ASME Journal of Turbomachinery, Vol. 113, pp. 42-51.